American Journal of Civil Engineering
2026, Vol. 14, No. 5, pp. 396–410
https://doi.org/10.11648/j.ajce.20261405.20

Research Article

Modelling the Compressive Strength of Bituminous Sand Concrete

John Ebipuakebina Agori[1, *], Solomon Ugwa Okoroafor[2], Christopher Onome Aruawamedor[1], Jeff Oba[3], Lucky Osiwime Umukoro[1], Eseha Anthony Enifome[3], Moses Ogheneruemu Utoyo[1], Daniel Osakwe[1], Charles Iboyi[1]

[1]Department of Civil Engineering, Delta State University, Abraka, Nigeria

[2]Department of Civil Engineering, Michael Okpara University of Agriculture, Umudike, Nigeria

[3]Department of Civil Engineering, Federal University of Technology, Owerri, Nigeria

Abstract

Global demand for river sand now outstrips natural replenishment, driving the search for sustainable alternatives. This study characterizes bituminous sand from bitumen deposits in Ondo State, Nigeria, as a substitute for river sand in concrete and develops regression and machine-learning frameworks to predict compressive strength. Aggregate characterization recorded effective sizes (D_{10}) of 0.123 mm (river sand) and 0.099 mm (bituminous sand), with uniformity coefficients of 3.959 and 4.495, indicating well-graded materials. Moisture contents averaged 72%, 60% and 8% for river sand, bituminous sand and granite; silt contents averaged 2.46% and 4.98%, against an 8% permissible limit. Specific gravities were 2.64, 2.60 and 2.70, bulk densities 1780, 1717 and 1677 kg/m^3, and water absorption 0.91%, 0.70% and 0.74% respectively. Using a grade M25 mix of ratio 1: 1: 2 (characteristic strength 25 N/mm^2 at 28 days, target 38 N/mm^2), BSC showed higher workability (slump 55 mm vs 30 mm, compacting factor 0.49 vs 0.46) and strength gain with curing age, from 9.38 N/mm^2 at 7 days to 15.35 N/mm^2 at 150 days, against 15.17-26.93 N/mm^2 for the control (36-43% differences). BSC density (2213 kg/m^3, 13.41 N/mm^2) was within 10% of the control (2462 kg/m^3, 22.32 N/mm^2), classifying BSC as normal-weight concrete, and water absorption stayed within the 10-15% band (averages 11.37% and 11.30%). Multi-model regression: the exponential curing-age model fitted the control best (R^2 = 0.8692) and the logarithmic model fitted BSC best (R^2 = 0.8008), with adequacy confirmed by F-statistics of 187.68 and 757.64 and a t-test (2.14 < 2.57). A five-stage machine-learning framework is then specified, benchmarked against ANN achieving R^2 = 0.894 with the lowest RMSE (5.192 MPa) on a 1234-record dataset. The results position bituminous sand as a technically viable, sustainable alternative fine aggregate with a data-driven strength-prediction route.

Keywords

Bituminous Sand, Bitumen Sand Concrete, Fine Aggregate, Compressive Strength, Regression Models, Machine Learning, Sustainable Concrete

*Correspondence: John Ebipuakebina Agori (agorious5@gmail.com)

Received: 2 October 2026; **Accepted:** 13 October 2026; **Published:** 29 October 2026

Copyright: © The Author(s), 2026. Published by Science Publishing Group. This is an **Open Access** article, distributed under the terms of the Creative Commons Attribution 4.0 License (http://creativecommons.org/licenses/by/4.0/), which permits unrestricted use, distribution and reproduction in any medium, provided the original work is properly cited.

1. Introduction

Concrete is the most frequently utilized building material in the world, with about 7.5 billion cubic metres produced annually at a growth rate of 6% [1]. Aggregates constitute approximately 70-80% of concrete volume, with fine aggregate representing about 40-50% of aggregate volume [2]. According to the United Nations Environment Programme, total demand for river sand could exceed 40 billion tons per year, more than twice the sediments carried by the world's rivers, while annual concrete production, estimated at 10 billion tons, is expected to rise to 18 billion tons by 2050, and global aggregate demand is projected to reach 50-55 billion tons by 2030 [2, 3]. With unregulated river sand mining altering river flow, increasing erosion and disrupting aquatic habitats, many regions now restrict extraction to conserve riverbeds [4], and demand for alternative fine aggregates has risen dramatically [5]; for developing economies, a dependable local substitute is a material-supply imperative. Substitution studies offer a route forward. Concrete with 30% sustainable sand gave the best strength result, with acceptable decreases at 50% replacement, significant reductions at 100%, and approximately 735 $\times 10^6$ tons of river sand preserved at 50% replacement [6]. Recommended limits include not more than 35% rock-based fines, 5-10% waste polymer fractions and 30% rice husk [7]. Industrial by-products, granulated blast-furnace slag and manufactured sand [8], industrial side streams [2], basalt and limestone cutting dust [4], and copper slag with recycled glass [6], represent a long-term approach to excessive river mining and by-product disposal.

Bituminous sands, Figure 1, are naturally occurring bitumen-impregnated sands, locally abundant but under-characterized in Nigeria, with Ondo State deposits occurring as soft, low-viscosity bitumen seepages within a belt about 12 km wide extending from Ijebu-Ode in Ogun State, through Ondo State, to Edo State, in the Upper Cretaceous sequence of the Abeokuta Formation of the eastern Dahomey Basin. Nigeria's reserves, estimated at about 42.47 billion tons, are ranked the second largest in the world, with most concentrated in Ondo State. Related Nigerian works found bituminous sand viable in sandcrete at 0-40% replacement, with strength increasing with curing age [9], and plain bituminous-sand concrete showing better workability than the control [10]. Reclaimed asphalt pavement, the material most chemically akin to bituminous sand, requires complete characterization [11]; it presents good freeze-thaw resistance [11], higher open porosity than natural-aggregate concrete [12], chloride permeability unaffected at up to 50% coarse-aggregate replacement [13], an average durability factor of 73% after 300 freeze-thaw cycles at 15-20% replacement [14], 30-50% replacement studied for highway base layers [15], and increased superplasticizer demand as fine aggregate [16]. Strength development and its prediction are equally critical. Water curing is the benchmark regime [17]; air curing reduces mid-age strength by up to 19%, while carbonation curing produces late-age gains of 7-12% at 182 days [18], and extended curing raised compressive strength by 39.4% [19]. Regression equations save time, capital and resources [20]. Machine-learning benchmarks show the artificial neural network achieving $R^2 = 0.894$ with the lowest root mean square error of 5.192 MPa on a 1234-record dataset [21], outperforming multiple linear regression, support vector machines and regression trees on 1030 samples [22], consistent with SonReb non-destructive assessment [23-25] and metaheuristic-guided error reductions from 9.3 to 4.8 MPa [26]. For high-strength concrete, extreme gradient boosting (XGBoost, $R^2 \approx 0.94$) outperformed other models [27], explainable artificial intelligence spanning eight models improves prediction transparency [28], and backpropagation adjusts neuron weights to minimize errors, decisive because concrete mix-strength relationships are significantly nonlinear [27].

Figure 1. *Bituminous sand.*

Current studies have not adequately assessed the effects of varying mix proportions, cement type, water-cement ratios and bituminous-sand content, so that effective utilization remains largely unexplored [7]. This study therefore predicts the compressive strength of bituminous sand concrete with the objectives of;

1) establishing the characteristics of the aggregates,
2) evaluating the fresh and hardened properties against a river-sand control,
3) developing models for compressive strength, and
4) testing the adequacy of the models, contributing the first engineering characterization of Nigerian bituminous sand as a concrete fine aggregate and a five-stage machine-learning framework positioned on that experimental baseline.

1.1. River Sand Depletion and Alternative Fine Aggregates

Sourcing alternatives to river sand has accelerated as construction activity depletes accessible reserves [57]. A systematic review of recycled and desert sand substitution reported that concrete prepared with 30% sustainable sand gives the best strength outcome relative to 100% river sand, with an acceptable decrease at 50% replacement and a significant reduction at 100%; at 50% replacement, approximately 735 × 10^6 tons of river sand would be preserved [6]. A subsequent systematic study of sustainable fine aggregate blended with supplementary cementitious materials found that manufactured sand can be tuned to enhance both mechanical performance and workability, that desert sand requires mix-design adjustment owing to its very fine particles (adequate compressive strength being achievable at 50% fine-aggregate substitution with about 20% supplementary cementitious material), and that combined waste incorporation can reduce CO_2 emissions by up to 50% [29]. A recent review of emerging fine-aggregate materials concluded that not more than 35% rock-based fines is suitable for river-sand replacement, that waste-polymer fractions should not exceed 5% (polyethylene terephthalate), 10% (polypropylene), 10% (expanded polystyrene) and 6% (melted plastic crushed fine aggregate), and that agro-waste such as rice husk should not exceed 30% to enhance strength and durability [7]. Industrial side streams including waste foundry sand, steel slag, stainless steel slag and iron slag have likewise been reviewed as self-compacting concrete fine aggregates, all producing significant changes in fresh and hardened properties [30]. Life-cycle assessment of recycled fine aggregate has shown that, at 28 days, mortar with 100% coarse sand achieved 25% higher compressive strength, and mortar with 100% fine sand 67% lower strength, than mortar with 100% recycled fine aggregate [31].

1.2. Bituminous Sand and Nigerian Bitumen Resources

Nigeria's bituminous sand reserves are estimated at about 42.47 billion tons, the second largest in the world with reported bitumen contents of 8-16% for Ilubirin samples and an overall range of 5-20% by weight for Nigerian deposits [32]. The engineering potential of Ondo State tar sand has been demonstrated for road work, where aggregate crushing value, aggregate impact value and Los Angeles abrasion were 28%, 23% and 38% respectively, and bitumen penetration was as low as 17 mm, indicating good resistance to rutting and bleeding [33]. Solvent-extraction studies of Okitipupa tar sand reported optimal bitumen yields of 9.07% at 75 ℃ in 4 h with n-hexane and 21.27% at 120 ℃ in 4 h with toluene [34]. Reviews of Nigerian bitumen upgrading further highlight the value of local deposits for sustainable infrastructure and the need for additive modification [35]. In concrete applications, bituminous sand has been shown to be viable in sandcrete at 0-40% replacement, with the 0% bituminous-sand/100% river-sand sample gaining the highest strength of 8.59 N/mm^2 at 28 days [9], and plain bituminous-sand concrete has exhibited better workability than the control, with strengths rising with curing age to a level suitable for grade C15 applications [10, 58].

1.3. Reclaimed Asphalt Pavement as a Bitumen-Bearing Aggregate

Because RAP is the material most chemically akin to bituminous sand, its behaviour offers the closest analogue. Complete characterization of RAP before use is mandatory if durable concrete is required, and RAP generally shows good freeze-thaw resistance, with lower frost resistance observed only in the most porous samples [11]. The strength and modulus reductions in RAP concrete have been linked to a larger, more porous interfacial transition zone and to the dominance of asphalt cohesion failure over asphalt-cement adhesion failure; replacement levels below 25% can be used in concrete pavements without significant change to the structural design, and field studies show 10-15% RAP performing comparably to conventional concrete [36]. Durability testing of structural concrete found that sorptivity decreased with increasing RAP content because of the hydrophobic nature of the aggregate, while water absorption was less affected and carbonation and chloride resistance were governed more by water/cement ratio and cement type than by RAP content [37]. RAP replacement of 25% and 50% has been shown to remain within limit values for concrete pavement, with high corrosion resistance [38], and systematic review confirms that RAP concrete can match conventional concrete mechanically while improving sustainability [39]. Where fine RAP is used as a sand substitute, a systematic reduction in compressive strength is observed as the fine-RAP percentage increases [40]; analogous work on bituminous road waste as a partial fine-aggregate replacement (10-30%, M30 grade) likewise targeted enhanced mechanical performance and sustainability [41].

1.4. Strength Development, Curing and Durability

Curing method and duration strongly govern strength development. Comparative studies rank complete immersion in water as producing the highest mean compressive strength, ahead of polyethylene membrane and gunny-bag curing, with sprinkling the least effective [17]; a parallel study reported a maximum 28-day compressive strength of 41.42 MPa under water-submergence curing [42]. Curing-condition research has shown that air curing impedes strength gain, affecting fly-ash concrete more than ordinary Portland cement concrete [43], while wet curing for as little as three days encourages sufficient strength growth with reduced shrinkage and cracking [44]. Extended curing has been shown to raise compressive strength from 18.5 to 25.8 MPa (a 39.4% gain) while re-

ducing water absorption from 6.45% to 5.65% (a 12.4% reduction) and improving split tensile strength from 2.05 to 2.65 MPa (29.3%) [19]. Particle-size distribution is itself a controlling variable: the gradation of standard sands, quantified by fineness modulus and uniformity coefficient directly affects the physical-mechanical properties of mortars [45].

1.5. Machine-Learning Prediction of Compressive Strength

ML has become a mainstream route to rapid strength estimation, [59]. An evaluation of eight popular ML models on a standard 1030-sample dataset found XGBoost to outperform all others in R^2 and RMSE, achieving 0.91 and 4.37 respectively [28], a result echoed by an XAI study in which XGBoost yielded the best-reported performance across eight models, interpreted through SHAP [28]. On 633 experimental records spanning compressive strengths of 6.27-79.99 MPa, the XGBoost regressor was again most reliable (R^2 = 0.95, RMSE = 3.06 MPa, MAE = 2.13 MPa), with multiple linear regression the least accurate (R^2 = 0.52, RMSE = 9.40 MPa) [46]. Multi-model comparisons of ANN, XGBoost and random forest have reported comparable, stable performance across all three [47]. In recycled-aggregate self-compacting concrete, an interpretable ML framework built on 400 experimental samples and eight input variables achieved XGBoost R^2 = 0.98 (RMSE = 2.95 MPa) in training and R^2 = 0.96 (RMSE = 3.25 MPa) in testing, with SHAP identifying superplasticizer, cement and cement strength as the dominant features (Almutairi, 2025). Across five gradient-boosting algorithms on 314 recycled-aggregate mixes, categorical gradient boosting reached the highest test R^2 of 92% [49], while for fibre-reinforced recycled aggregate concrete the gradient-boosted regression tree model achieved R^2 = 0.95 (training) and 0.83 (testing) for splitting tensile strength [50]. Ensemble approaches on 301 recycled-aggregate self-compacting specimens and 18 input variables reached R^2 = 0.963, RMSE = 3.321 MPa and MAE = 2.506 MPa, with specimen age the dominant predictor [51]; and ML models have predicted multi-recycled aggregate concrete strength to $R^2 > 0.9$ even without advanced techniques [52]. Explainable ML has also been applied to fly-ash-GGBS geopolymer concrete, integrating strength, durability and carbon efficiency with SHAP interpretation [53]. This body of work establishes both the predictive power of ML for concrete strength and the importance of interpretability in deployment, the gap the present study addresses for bituminous sand concrete.

2. Materials and Methods

2.1. Materials

The constituent materials were ordinary Portland cement, river sand (control fine aggregate), bituminous sand, crushed granite coarse aggregate (10 mm and 20 mm nominal sizes), and clean mixing water free of salt, oil, acid, injurious alkali and vegetable matter. The bitumen content of the bituminous sand was determined by the cold solvent extraction method using a centrifuge extractor and trichloroethylene in accordance with ASTM D4-86 (2018). Laboratory tests were carried out at the engineering concrete laboratory of the Federal University of Technology, Owerri.

2.2. Methods

The experimental program followed a systematic eight-step methodology involving material sourcing, aggregate characterization, M25 mix design (1: 1: 2, 0.60 w/c), 150 mm cube specimen preparation, fresh property testing, water curing up to 150 days, hardened property evaluations, and final data analysis using regression and machine learning frameworks as shown in Figure 2.

2.2.1. Aggregate Characterization Tests

Sieve analysis: The engineering properties of the river sand, bituminous sand, and coarse aggregates were evaluated through systematic particle size distribution analysis. Using the resulting semi-logarithmic gradation curves, the key geometric parameters, specifically the coefficient of curvature and the uniformity coefficient were mathematically determined to characterize the grading structure of the fine aggregates. The coefficient of curvature and uniformity coefficient for fine aggregates were calculated from, Equations (1) and (2):

$$Cc = \frac{D_{30}^2}{D_{60} \times D_{10}} \quad (1)$$

$$C_u = \frac{D_{60}}{D_{10}} \quad (2)$$

where D_{10} is the effective particle size (10% of particles finer, 90% coarser), D_{30} the size at which 30% are finer, and D_{60} the size at which 60% are finer and 40% coarser.

Moisture content. Natural moisture contents of the sands and coarse aggregates were determined prior to mixing because they affect the proportion of mixing water needed to achieve the desired water/cement ratio, in accordance with ASTM C70 (2020), Equation (3):

$$MC \ (\%) = \frac{W_w - W_d}{W_d} \times 100 \quad (3)$$

where: MC = moisture content (%), W_w = weight of the wet sample, W_d = weight of the dry sample,

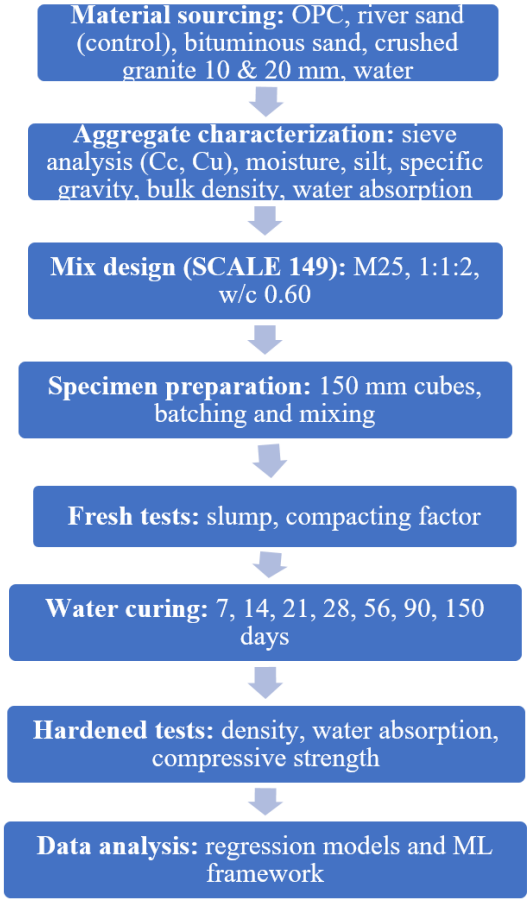

Figure 2. *Flowchart of the experimental methodology for concrete material characterization, mix design, testing, and data analysis of the study.*

Silt content. Silt content was determined volumetrically, silt being material finer than 150 microns, excessive quantities of which reduce cement bonding and concrete strength, Equation (4):

$$Silt\ \ (\%) = \frac{h_1}{h_2} \times 100 \tag{4}$$

where h_1 is the silt layer thickness and h_2 the height of sand plus silt.

Specific gravity, bulk density and water absorption. Specific gravity and bulk density were determined in accordance with ASTM C-29 (2017) guidelines and evaluated against ASTM C 128-22 (2023), Equations (5) and (6):

$$\rho_b = \frac{M_3}{V} \tag{5}$$

$$WA\ \ (\%) = \frac{|W_2 - W_1|}{W_1} \times 100 \tag{6}$$

where: ρ_b = bulk density, M_3 = mass of the sample, V = volume of the sample, WA = water absorption (%), W_1 = initial/dry weight of the sample, W_2 = final/saturated weight of the sample, $|W_2 - W_1|$ = absolute difference between the two weights.

2.2.2. Mix Design

Concrete mix design was performed using SCALE 149 SOFTWARE, which yielded the characteristic concrete strength of 25 N/mm^2 at 28 days, 5% defectives, standard deviation of 8 N/mm^2, slump ranges of 10-30 mm and specific gravity of coarse aggregate of 2.70. The design calculations are reproduced as the worked example below, and the resulting quantities in Figure 3, Table 1. The mix ratio used was 1: 1: 2 of cement: fine aggregate: coarse aggregate, for crushed aggregates not more than 20 mm as per BS EN 206 (2021).

Table 1. *Mix design quantities.*

Constituent	Per m^3 (kg)	Per trial mix of 0.01 m^3, 3 cubes (kg)
Cement	285	2.85
Water	170	1.7
Fine aggregate	620	6.2
Coarse aggregate (10 mm)	460	4.6
Coarse aggregate (20 mm)	925	9.25

Note: Cement content: kg/m^3 at a free-water/cement ratio of 0.6; Wet density: 2460 kg/m^3; Coarse aggregate content: 2005 - 620 = 1385 kg/m^3

Figure 3. *Standard block diagram of the methodology for M25 concrete mix design, aggregate characterization and material selection.*

2.2.3. Specimen Preparation and Curing

Concrete cube specimens were prepared, tested and cured in accordance with BS EN 12390-3 (2019), with a loaded area of 22,500 mm^2 (150 mm cubes). Cubes were cured for 7, 14, 21, 28, 56, 90 and 150 days, then tested for slump, compacting factor, density, water absorption and compressive strength.

The compacting factor was obtained as the ratio of the density during the test to the density of fully compacted concrete; as a fraction, the higher the value the more workable the concrete, and the British Standards Institution states that compacting factor is always less than one, Equation (7):

$$CF = \frac{\rho_{partial}}{\rho_{full}} \quad (7)$$

where: CF = compaction factor, $\rho_{partial}$ = density of the partially compacted material, ρ_{full} = density of the fully compacted material.

2.2.4. Compressive Strength Test

Average crushing loads were taken for each set of cubes and the compressive strength evaluated using, Equation (8).

$$f_{cu} = \frac{P}{A} \quad (8)$$

where, P is the average compressive load at failure (N) and A the cross-sectional area of the cube in mm^2. The water absorption test procedure immersed each specimen in water for 24 hours, and absorption was expressed as a percentage of the initial weight of the sample.

2.2.5. Statistical Modelling Methodology

Model development followed five steps:

1) Relevant data were gathered on compressive strength with parameters including curing time, mix proportions and related factors;
2) Data were cleaned and pre-processed (missing values, outliers, consistency);
3) The dataset was prepared for analysis using an Excel Regression Spreadsheet, identifying independent variables likely to affect compressive strength including type of sand, water-cement ratio and curing conditions;
4) Training and testing sets were separated to develop the predictive model and evaluate performance; and
5) Suitable regression models, both linear and multiple were employed to account for the complexity of relationships among the variables. The four model families fitted to curing age take the forms Equations (9-12):

$$f(x) = ax + b \quad (linear) \quad (9)$$

$$f(x) = a\ ln\ ln\ \ (x) + b \quad (logarithmic) \quad (10)$$

$$f(x) = ae^{bx} \quad (exponential) \quad (11)$$

$$f(x) = ax^2 + bx + c \quad (polynomial) \quad (12)$$

where:

f(x) = Dependent variable, the IDF empirical parameter (a or b) being regressed against return period, x = Independent variable, the return period (T) (years), a = First regression coefficient (slope in the linear model; multiplier of (ln(T)) in the logarithmic model; coefficient of the exponential term in Equation (11); leading quadratic coefficient in Equation (12), b = Second regression coefficient (intercept in Equations (9) and (10); exponent multiplier in Equation (11); linear coefficient in Equation (12), c = Third regression coefficient, intercept (constant term) in the polynomial model only (Equation (12), ln(x) = Natural logarithm of the return period (T), e = Base of the natural logarithm (≈ 2.7183).

Adequacy of the compressive strength models was tested with the statistical F-test and Student's t-test, assessed via R^2, the standard error of each model, and visual residual inspection, at the 0.05 significance level. Correlation matrices established the significance levels of the different variables for both concretes.

2.2.6. Machine-learning Framework Specification

The machine learning framework used in this study follows the ANN model development process is illustrated in Figure 4. This comprehensive framework outlines five sequential stages spanning from data collection and preprocessing to network design, partitioning, and final model evaluation. The five-stage framework, presented in Figure 5, proceeds as follows: (i) Min-Max standardization to (−1, 1) per Eq. (13); (ii) feed-forward network construction per Eq. (14), with weight selection based on minimum performance measures such as MSE; (iii) training-validation-testing partitioning; (iv) evaluation via MSE, R, MAD, RMSE, r and MAPE [22]; and (v) XAI interpretation of the trained networks [28].

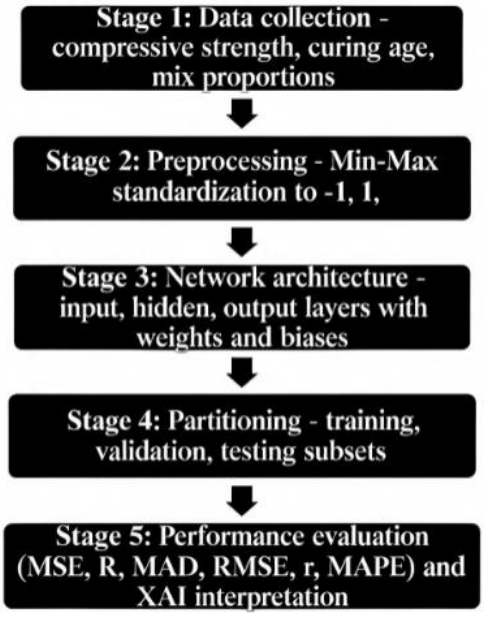

Figure 4. *Five-stage ML framework block diagram. a) Data standardization.*

To ensure model stability, the raw dataset was normalized

to a range of (−1, 1) using the Min-Max algorithm to minimize differences in variable scales and facilitate effective network learning, Equation (13):

$$x_{norm} = \frac{2\ (x - x_{min})}{x_{max} - x_{min}} - 1 \quad (13)$$

where: x_{norm} is the normalized value of xxx, scaled to the range [−1, 1], x is the original input value, x_{min} is the minimum value in the original data range, x_{max} is the maximum value in the original data range, $x_{max} - x_{min}$ is the range of the original data.

b) Network architecture. The ANN consists of an input layer, hidden layers and an output layer, each layer comprising processing units with weight and bias parameters; the activation function transfers data from the hidden layer to the output layer, and the neuron's output y is a nonlinear sum of the inputs, Equation (15):

$$y_j = f\left(\sum_i w_{ij} x_i + b_j\right) \quad (14)$$

where: y_j is the output of neuron j, f(·) is the activation function applied to the neuron's weighted input, ∑i denotes the summation over all input features or neurons indexed by I, w_{ij} is the weight connecting input x_i to neuron j, x_i is the i-th input value, b_j is the bias term for neuron j, $\sum_i w_{ij} x_i + b_j$ is the total weighted input to neuron j before activation.

c) Partitioning. The normalized dataset is divided into training, validation and testing subsets.

d) Performance criteria. The statistical parameters adopted for exploring the presentation of the ANN model are the mean square error and correlation coefficient (R), alongside mean absolute deviation, root mean square error, coefficient of correlation and mean absolute percentage error [22], Equations (15) and (16):

$$MSE = \frac{1}{N} \sum_{i=1}^{N} (S_i - S_i')^2 \quad (15)$$

$$RMSE = \sqrt{\left(\sum_{i-1}^{N} (S_i - S_i')^2\right)} \quad (16)$$

where: MSE is the mean squared error, N is the total number of data points or samples. S_i is the actual or observed value for the i-th sample, S_i' is the predicted value for the i-th sample, $S_i - S_i'$ is the prediction error for the i-th sample, $(S_i - S_i')^2$ is the squared prediction error.

$\sum_{i=1}^{N} (S_i - S_i')^2$ is the sum of squared errors over all N samples, RMSE is the root mean squared error.

The square root converts the summed squared error back to the original units of S_i.

3. Results and Discussion

3.1. Aggregate Characterization

The physical, index, and engineering properties of the selected aggregates were evaluated to determine their suitability for concrete production, with the consolidated characterization parameters summarized in Table 2.

Table 2. *Index and engineering properties of the aggregates.*

Property	River sand	Bituminous sand	Granite (coarse)
Effective size, D_{10} (mm)	0.123	0.099	4.722
Uniformity coefficient, C_u	3.959	4.495	2.884
Fineness modulus	4.78	4.47	5.39
Mean moisture content (%)	72	60	8
Mean silt content (%)	2.46	4.98	-
Specific gravity (g/cm^3)	2.64	2.60	2.70
Bulk density (kg/m^3)	1780	1717	1677
Water absorption (%)	0.91	0.70	0.74

From the particle size distribution curves, the fine aggregates predominantly pass through finer sieves, indicating a relatively well-graded material, for particles finer than 0.15 mm through to 2.36 mm (river sand) and from 1.18 mm to 2.36 mm (bituminous sand); the river sand curve is smooth and steep, suggesting balanced size distribution, whereas the bituminous sand grades gradually to 0.6 mm and lesser sizes. The effective size (D_{10}) is 0.123 mm for river sand and 0.099 mm for bituminous sand, required for cohesive concrete mixes with reduced voids, and the uniformity coefficients of 3.959 and 4.495 indicate high-strength mixes with improved bonding. Worked checks of Eq. (2) confirm D_{60} = 0.487 mm (river

sand) and 4.495 × 0.099 = 0.445 mm (bituminous sand); for coarse aggregates, D_{10} = 4.722 mm and C_u = 2.884, advantageous for higher concrete strength through interlocking of larger aggregates. The fineness modulus values of 4.78, 4.47 and 5.39 for river sand, bituminous sand and coarse aggregate respectively align closely with industrial standards, and the particle size distribution falls within recommended ranges, enhancing compactness by filling voids, reducing segregation and ensuring uniform matrix distribution.

Moisture content was 72% for river sand, 60% for bituminous sand and 8% for coarse aggregate, impacting workability, compaction and durability; adequate moisture control during batching and mixing was therefore employed. Silt content for the river sand was 2.46%, characteristic of an adequate clay content relative to the 8% permissible limit, indicating low segregation, good finishing and increased strength. The bituminous sand averaged 4.98% (trials 5.04%, 4.78% and 5.13%), within standard requirements, indicating good cohesion, adhesion and moisture. Specific gravity was 2.64 g/cm^3, 2.6 g/cm^3 and 2.7 g/cm^3 for river sand, bituminous sand and coarse aggregate respectively, of appropriate quality and suitable for use. Bulk density was 1780 kg/m^3 for river sand, 1717 kg/m^3 for bituminous sand (trials 1700, 1680 and 1770 kg/m^3) and 1677 kg/m^3 for granite (trials 1690, 1660 and 1680 kg/m^3), conforming to normal-weight concrete standards. Water absorption values of 0.91%, 0.70% and 0.74% for river sand, bituminous sand and granite respectively demonstrate non-porous aggregates free of reduced compressive strength, increased permeability and freeze-thaw susceptibility. These values compare favourably with RAP, where complete characterization is mandatory [12] and fine RAP introduced additional pores and increased superplasticizer demand [16], giving raw bituminous sand a distinct advantage.

3.2. Fresh Properties

The workability and consistency parameters of the fresh concrete mixtures were evaluated immediately after mixing, with the corresponding slump values and compacting factors presented in Table 3.

Table 3. *Slump and compacting factor results.*

Sample	Slump (mm)	Degree of workability	Compacting factor	Remark
Control	30	Low	0.46	Very Low
Bituminous sand concrete	55	Medium	0.49	Very Low

Control concrete recorded a slump of 30 mm (low workability) against 55 mm (medium workability) for BSC, and compacting factors of 0.46 and 0.49 respectively. The compacting factor values reflect relatively low workability, with the aggregates moderately distributed and the voids in the mixture typically average. The superior placeability of BSC is consistent with recent findings that bituminous sand concrete has better workability than the control [10].

3.3. Compressive Strength Development

The mechanical performance of the concrete mixtures was tracked across multiple curing durations to evaluate structural integrity over time. Table 4 presents a comparative summary of the compressive strength development for both the bituminous sand concrete (BSC) and the conventional river sand control mix.

Table 4. *Comparison of compressive strengths of BSC and control concrete.*

Curing age (days)	BSC (N/mm^2)	Control (N/mm^2)	Difference (N/mm^2)	% difference
7	9.38	15.17	5.79	38
14	10.74	17.11	6.37	37
21	12.83	20.66	7.38	36
28	15.02	24.70	9.68	40
56	15.22	25.76	10.54	41
90	15.32	25.88	10.56	41

Curing age (days)	BSC (N/mm^2)	Control (N/mm^2)	Difference (N/mm^2)	% difference
150	15.35	26.93	11.58	43

The mechanical performance evaluation revealed that the compressive strength of the Bituminous Sand Concrete increased progressively with curing age, mirroring the behavioural trends of conventional Ordinary Portland Cement concrete despite a slower initial rate of strength gain up to 28 days. A typical worked validation of the mathematical models, such as the BSC 7-day cube featuring an average mass of 7.24 kg and an average failure load of 211.33 kN, yielded a calculated density of 2145.19 kg/m^3 and a corresponding compressive strength of 9.38 N/mm^2. This aligns directly with the baseline analysis metrics established for the control mix at 150 days using the same standard cube volume (m^3) and density (kg/m^3) parameters. Quantitatively, the control concrete achieved a minimum compressive strength of 15.17 N/mm^2 at 7 days, which advanced to averages of 20.66 N/mm^2 at 21 days, 25.76 N/mm^2 at 56 days, and reached a terminal maximum value of 26.93 N/mm^2 at 150 days. In comparison, the BSC mixtures exhibited compressive strengths of 9.38 N/mm^2 at 7 days, 12.83 N/mm^2 at 21 days, 15.22 N/mm^2 at 56 days, and 15.35 N/mm^2 at 150 days. Chronological tracking verified a matching reported strength difference threshold of 43% between the configurations. Specifically, the control concrete demonstrated sequential strength increments of 36% over the first 21 days, 61% at 56 days, and 66% by 150 days, yielding a mean progression rate of 22% across the entire evaluation matrix. Conversely, the BSC mixtures showed corresponding strength expansions of 37%, 53%, and 54% across identical intervals, maintaining a mean progression rate of 18%. This marginal 4% variability in strength development behaviour is directly attributable to the chemical interaction boundaries between the cement matrix and the native bitumen fraction. While this phenomenon limits early-stage hydration, the subsequent strength development remains gradual and continuous. Consequently, by 56 days of curing, the absolute strength profiles of the sustainable BSC variations began to converge closely with the parallel improvement curves established by the conventional river sand control mix. The timeline of mechanical performance across the entire testing period is illustrated in Figure 5, which graphically maps the compressive strength development up to 150 days using the data compiled in Table 4.

This strength-age behaviour is consistent with the curing literature: water curing provides steady strength development and serves as a performance benchmark, while interrupted curing produces significant mid-age strength reductions of up to 19% [17, 18], and the decelerating character of the curve underlies the logarithmic fits of Section 4.6, in line with carbonation-driven pore refinement and matrix densification at later ages [18].

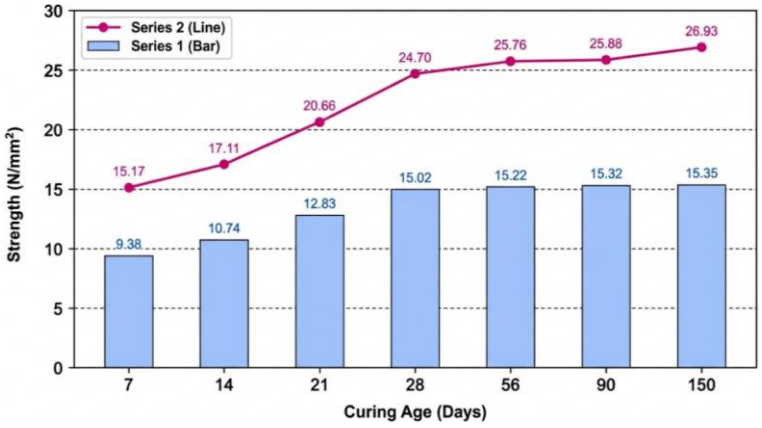

Figure 5. Compressive strength development to 150 days.

3.4. Density and Structural Classification

The typical BSC density obtained was 2213 kg/m^3 with a compressive strength of 13.41 N/mm^2, compared with 2462 kg/m^3 and 22.32 N/mm^2 for the control; the difference of less than 10% in density and around 40% in strength indicated that the bituminous concrete is suitable for normal weight (structural) structures. The designed wet density of 2460 kg/m^3 from the mix design is essentially recovered in the measured control hardened density (2482.96 kg/m^3 at 150 days), confirming batching fidelity. A 7-day BSC density of 2145.19 kg/m^3 was recorded in the strength tests.

3.5. Durability: Water Absorption

The durability performance of the hardened concrete mixtures was monitored across all testing intervals, with the percentage water absorption at the different curing ages summarized in Table 5.

Table 5. *Percentage water absorption of the river sand (control) and bituminous sand concretes at each curing age, with the average values used to assess durability and moisture resistance.*

Curing age (days)	River sand concrete (%)	Bituminous sand concrete (%)
7	10.58	11.46
14	13.18	12.40
21	11.34	12.13
28	12.62	11.16
56	12.83	11.55
90	9.34	10.09
150	9.67	10.34
Average	11.37	11.30

These values fall within the general standard range of water absorption percentages, typically set between 10 to 15% for normal weight concrete, establishing a crucial connection between the test outcomes and the expected performance of the concrete; the ability to maintain water absorption within this range over different curing periods is indicative of the concrete's durability and resistance to water. A mathematical validation of the fluid transport dynamics was performed using the experimental datasets, confirming the worked check of Eq. (6) for the river sand concrete at 7 days as tabulated. The resulting average water absorption values of 11.37% for the conventional river sand concrete and 11.30% for the alternative mixture demonstrate robust durability indicators and reliable moisture resistance across both design matrices. These uniform transport properties provide clear assurance that both concrete variants satisfy standard structural specifications necessary to maintain microstructural integrity throughout their anticipated service life. This performance corresponds directly with established multi-method pore-structure evidence demonstrating that internal porosity and localized water retention mechanisms fundamentally govern long-term concrete durability [54]. Furthermore, these trends match parallel findings from the M15 baseline model, where extended curing protocols effectively reduced concrete water absorption from 6.45% to 5.65%, representing a 12.4% total reduction, while simultaneously increasing net compressive strength by 39.4% [19].

3.6. Regression Models and Statistical Adequacy

Beyond the isolated curing-age trendlines, the multi-variable regression analysis generated comprehensive mathematical models to predict structural performance. Distinct model structures were established for the river sand concrete and the bituminous sand concrete, defining compressive strength as a function of operational design features, including curing age (a), cement content (b), fine aggregate volume (c), and coarse aggregate fraction (d). To determine the most accurate mathematical relationship between concrete maturity and compressive strength, different regression types were evaluated. Table 6 presents the curing-age regression models and coefficients of determination (R^2) for the control (river sand) concrete, comparing exponential, linear, logarithmic, and polynomial fits.

Table 6. *Curing-age regression models and coefficients of determination (R2) for the control (river sand) concrete, comparing exponential, linear, logarithmic and polynomial fits.*

Model type	Equation	R2
Exponential	0.282e^(0.2136x)	0.8692
Linear	8.4178x − 135.56	0.584
Logarithmic	167.71ln(x) − 464.96	0.5436
Polynomial	1.859x2 − 70.165x + 657.13	0.7762

3.7. Regression Models and Statistical Adequacy

Beyond the isolated curing-age trendlines, the multi-variable regression analysis generated comprehensive mathematical models to predict structural performance. Distinct model structures were established for the river sand concrete and the bituminous sand concrete (BSC), defining compressive strength as a function of operational design features, including curing age (a), cement content (b), fine aggregate volume (c), and coarse aggregate fraction (d). Various mathematical functions were evaluated to determine the best relationship between curing time and strength development.

Table 7. *Curing-age regression models and R^2 values for the control concrete.*

Model type	Equation	R^2
Exponential	$0.282e^{(0.2136x)}$	0.8692
Linear	$8.4178x - 135.56$	0.584
Logarithmic	$167.71\ln(x) - 464.96$	0.5436
Polynomial	$1.859x^2 - 70.165x + 657.13$	0.7762

Table 8. *Curing-age regression models and coefficients of determination (R2) for the bituminous sand concrete, comparing exponential, linear, logarithmic and polynomial fits.*

Model type	Equation	R^2
Exponential	11.505e^(0.0026x)	0.4539
Linear	0.0331x + 11.677	0.4764
Logarithmic	2.0644ln(x) + 6.1839	0.8008
Polynomial	$-0.0007x^2 + 0.1369x + 9.6425$	0.7819

The curing-age regression models and their R^2 values for both concretes are compared in Tables 7 and 8, and the corresponding regression statistics are summarized in Table 9.

Table 9. *Regression statistics for the compressive strength of the control and bituminous concretes.*

Statistic	Control	BSC
Multiple R	0.9850	0.9826
R Square	0.9702	0.9655
Adjusted R Square	−0.0497	−0.0576
Standard error	0.8508	0.4559
Observations	7.0000	7.0000
ANOVA F (df 5, 3)	48.8394	41.9178
Significance F	0.0000	0.0000
Intercept (t Stat, p)	10.9017 (7.0852, 0.0058)	7.3583 (8.9237, 0.0030)
Curing age coefficient (t Stat, p)	−0.0717 (−3.4894, 0.0398)	−0.0479 (−4.3570)

The best-fitted trend for the control and bituminous concretes was the logarithmic. Standard errors show that, for bituminous concrete, the linear models for curing age and cement provide the best fit; all four models fit the fine aggregate variable similarly, whereas the coarse aggregate variable posed issues with the linear and logarithmic models, the exponential and polynomial variants performing better. The F-statistics were very large, approximately 187.68 and 757.64 for compressive strength and curing age, indicating significant differences for both mixes. The calculated t-statistic of 2.14 is less than the critical value of 2.57, so the null hypothesis is accepted and the model deemed adequate. The p-values support this conclusion; although both concretes exhibit significant mean differences between curing age and compressive strength, no significant difference in observed parameters exists between the concrete types. Curing age is therefore the most relevant factor governing adequate strength, mirroring ANOVA-based practice in related concrete research [55] and the decelerating strength-age trajectory under prolonged curing [18].

3.8. Machine-learning Framework

The adequacy-verified MLR equations constitute the transparent baseline for ML benchmarking. The modeling envelope was rigorously benchmarked across 1,030 preprocessed data samples. The dataset was initially split into a 70% training and 30% testing partition, with the ANN training matrix further sub-allocated into 70% training, 15% validation, and 15% testing subsets. Ultimately, the ANN achieved superior predictive accuracy and computational efficiency, outperforming multiple linear regression, support vector machines, and regression tree alternatives. Furthermore, across an independent set of 1,234 compressive strength evaluations modulated by eight operational predictor variables, the support vector regression model generated a coefficient of determination of $R^2 = 0.897$ (RMSE = 6.535 MPa), while the gradient boosting framework achieved an $R^2 = 0.885$ (RMSE = 5.437 MPa). Comparatively, the parallel ANN design converged at an $R^2 = 0.894$ alongside the absolute lowest root-mean-square error of 5.192 MPa, validating the exceptional capacity of neural network architectures to characterize high-dimensional dataset non-linearities and preserve target response variances [21].

For high-strength concrete, XGBoost ($R^2 \approx 0.94$) outperformed other models on a dataset of 167 mix records [27]. Because the mixture-strength relationship is significantly nonlinear, making an adequate single regression expression challenging [27], ML implementation accelerates strength determination, reducing testing costs [27], and for in-situ assessment, the SonReb literature confirms the best performance of the ANN approach [24, 25], with ANN enabling practical strength evaluation where mix records are unavailable [56]. XAI techniques should accompany deployment to improve transparency and interpretability of the strength predictions [28, 48].

4. Conclusions

4.1. Key Findings

Bituminous sand from Ondo State is well graded (C_u = 4.495 vs 3.959 for river sand), with specific gravity 2.60, bulk density 1717 kg/m^3, water absorption 0.70% and silt content 4.98% within the 8% limit, confirming its suitability as a fine aggregate. In fresh state, BSC was more workable than the river-sand control (slump 55 mm vs 30 mm; compacting factor 0.49 vs 0.46). Under water curing, BSC strength grew steadily with age, reaching 15.35 N/mm^2 at 150 days against 26.93 N/mm^2 for the control (a 43% difference at 150 days), and its density (2213 kg/m^3 at 13.41 N/mm^2) fell within 10% of the control (2462 kg/m^3 at 22.32 N/mm^2), classifying it as normal-weight concrete. Water absorption remained within the 10-15% band (averages 11.37% and 11.30%). Among the multi-model regressions, the logarithmic model best fitted BSC (R^2 = 0.8008) and the exponential model best fitted the control (R^2 = 0.8692); adequacy was confirmed by F-statistics of 187.68 and 757.64 and by a t-test (2.14 < 2.57). The benchmark-supported ANN framework (R^2 = 0.894; RMSE 5.192 MPa) provides a reliable data-driven prediction route.

4.2. Practical Implications

The results position bituminous sand as a technically viable, sustainable fine aggregate for normal-weight concrete, particularly in hybrid and non-structural applications where the strength penalty relative to river sand is tolerable. Because the material is locally abundant in Ondo State and its processing does not require the energy-intensive crushing associated with manufactured sand, its use can reduce pressure on riverbeds, lower transport-related emissions and support circular-economy objectives in the Nigerian construction sector. The developed regression models and the five-stage ML framework give engineers a practical means of estimating compressive strength from curing age and mix parameters, reducing the number of destructive tests required during mix design and quality control.

4.3. Limitations

The study evaluated only two mixes across seven curing ages (n = 7), so the regression and ML models are based on a small dataset that increases the risk of overfitting and limits generalization. The experimental programme covered a single cement type, a single water/cement ratio and one grade (M25), and durability was assessed only through water absorption; long-term durability indicators such as chloride penetration, carbonation and freeze-thaw resistance were not investigated.

4.4. Future Work

Future work should (i) expand the dataset and train the ANN on augmented BSC datasets to improve robustness and generalization, incorporating larger benchmarks of approximately 1,030 records; (ii) extend the framework to additional mix proportions, cement types and water/cement ratios; (iii) evaluate long-term durability performance of BSC; and (iv) pair the predictive models with explainable-AI interpretation to improve transparency for deployment in practice.

Abbreviations

ANN	Artificial Neural Network
ASTM	American Society for Testing and Materials
BS EN	British Standard European Norm
BSC	Bituminous Sand Concrete
Cc	Coefficient of Curvature
CF	Compacting Factor
C_u	Uniformity Coefficient
D_{10}	Effective Particle Size (10% Finer)
D_{30}	Particle Size at Which 30% Are Finer
D_{60}	Particle Size at Which 60% Are Finer
MAD	Mean Absolute Deviation
MAPE	Mean Absolute Percentage Error
MC	Moisture Content
ML	Machine Learning
MLR	Multiple Linear Regression
MSE	Mean Squared Error
OPC	Ordinary Portland Cement
ORCID	Open Researcher and Contributor ID
R	Correlation Coefficient
R^2	Coefficient of Determination
RAP	Reclaimed Asphalt Pavement
RMSE	Root Mean Square Error
SVR	Support Vector Regression
SVM	Support Vector Machine
WA	Water Absorption
XAI	Explainable Artificial Intelligence
XGBoost	Extreme Gradient Boosting

Author Contributions

John Ebipuakebina Agori: Methodology, Project administration, Supervision, Writing – review & editing

Solomon Ugwa Okoroafor: Validation, Writing – original draft

Christopher Onome Aruawamedor: Software

Jeff Oba: Formal Analysis

Lucky Osiwime Umukoro: Data curation

Eseha Anthony Enifome: Funding acquisition, Resources

Moses Ogheneruemu Utoyo: Conceptualization

Daniel Osakwe: Visualization

Charles Iboyi: Investigation

Conflicts of Interest

The authors declare no conflicts of interest.

References

[1] Saha, A. K., Khan, Md. N. N., & Sarker, P. K. (2018). Value added utilization of by-product electric furnace ferronickel slag as construction materials: A review. Resources Conservation and Recycling, 134, 10-24. https://doi.org/10.1016/j.resconrec.2018.02.034

[2] Perumal, P., Gouriou, C., Adesanya, E., Mistri, A., & Illikainen, M. (2024). Sustainable application of industrial side streams as alternative fine aggregates for cement mortar. Innovative Infrastructure Solutions, 9(1). https://doi.org/10.1007/s41062-023-01334-z

[3] Bashir, M. T., Lal, R., Saifullah, H., Almutairi, A., Sikandar, M. A., Khan, Md. M. H., & Ounaies, W. (2026). A unified decision-oriented framework for sustainability assessment of electronic waste and recycled rubble aggregate concretes. Scientific Reports, 16(1). https://doi.org/10.1038/s41598-026-48896-3

[4] Awad, M. T., Shaqadan, A., Al-Adwan, J., & Maraqa, F. (2023). Recycling of Basalt and Limestone Cutting Dust in Concrete Mix Design. Civil Engineering Journal, 9(5), 1173-1186. https://doi.org/10.28991/cej-2023-09-05-010

[5] Dinh, H. L., Liu, J., Ong, D. E. L., & Doh, J. H. (2022). A sustainable solution to excessive river sand mining by utilizing by-products in concrete manufacturing: A state-of-the-art review. Cleaner Materials, 6, 100140. https://doi.org/10.1016/j.clema.2022.100140

[6] Akhtar, M. N., Bani-Hani, K. A., Malkawi, D. A. H., & Albatayneh, O. (2024). Suitability of sustainable sand for concrete manufacturing - A complete review of recycled and desert sand substitution. Results in Engineering, 23, 102478. https://doi.org/10.1016/j.rineng.2024.102478

[7] Sanusi, A., Ndububa, E. E., Amuda, A. G., Obianyo, I. I., Ahmed, A., Adeleke, W. A., Gunat, M. B., Abidemi, S. O., & Mambo, A. D. (2026). Replacing river sand in concrete: a review of emerging sustainable fine aggregate materials. Discover Sustainability, 7(1). https://doi.org/10.1007/s43621-026-02686-z

[8] Impa, K. A., Sachin, K. C., Abhishek, R., Bekkeri, G. B., Shetty, K. K., & Shashikumara, S. R. (2024). Experimentation on triple-blended concrete with manufactured sand replaced by granulated blast furnace slag for fine aggregates. Innovative Infrastructure Solutions, 9(4). https://doi.org/10.1007/s41062-024-01409-5

[9] Ezenkwa, C. S., Ede, A. N., Ogbaga, C. K., & Ogagaoghene, O. E. (2024). Utilization of Bituminous Sand in the Production of Eco-friendly Sandcrete for Sustainable Construction. IOP Conference Series Earth and Environmental Science, 1342(1), 12019. https://doi.org/10.1088/1755-1315/1342/1/012019

[10] Ezenkwa, C. S., Onwuka, D. O., Okere, C. E., Arimanwa, J. I., & Onwuka, S. U. (2025). Compressive strength and statistical investigation of concrete made with bituminous sand. International Journal of Science and Research Archive, 14(3), 417-429. https://doi.org/10.30574/ijsra.2025.14.3.2431

[11] Masi, G., Michelacci, A., Manzi, S., & Bignozzi, M. C. (2022). Assessment of reclaimed asphalt pavement as recycled aggregate for concrete. Archivio Istituzionale Della Ricerca, 341, 127745. https://doi.org/10.1016/j.conbuildmat.2022.127745

[12] Masi, G., Michelacci, A., Manzi, S., Esposti, A. D., Pascale, B., Bònoli, A., & Bignozzi, M. C. (2023). Performance and environmental analysis of Reclaimed Asphalt Pavement concrete produced in industrial environment (pp. 2831-2838). https://doi.org/10.1201/9781003323020-344

[13] Thomas, R. J., Fellows, A. J., & Sorensen, A. D. (2018). Durability Analysis of Recycled Asphalt Pavement as Partial Coarse Aggregate Replacement in a High-Strength Concrete Mixture. Journal of Materials in Civil Engineering, 30(5). https://doi.org/10.1061/(asce)mt.1943-5533.0002262

[14] Abut, Y., & Yıldırım, S. T. (2019). An investigation on the durability properties of RAP-containing roller compacted concrete pavement. European Journal of Environmental and Civil Engineering, 26(2), 802-818. https://doi.org/10.1080/19648189.2019.1679672

[15] Xu, W., Li, W., & Ji, Y. (2021). Mechanical Behavior Investigation of Reclaimed Asphalt Aggregate Concrete in a Cold Region. Materials, 14(15), 4101. https://doi.org/10.3390/ma14154101

[16] Nehari, A., Amer, A. A. M., Mostefa, A. H., Safer, O., Salhi, M., Abdoun, M., & Nabil, G. (2024). The influence of fine recycled asphalt pavement aggregates on the properties of self-compacting mortar in fresh and hardened state. Studies in Engineering and Exact Sciences, 5(2). https://doi.org/10.54021/seesv5n2-440

[17] Uzoka, C., & Imarhiagbe, A. (2025). Effect of Curing Duration and Methods on Concrete Compressive Strength of Concrete. Nile Journal of Engineering and Applied Science, 729-739. https://doi.org/10.5455/njeas.286654

[18] Osadola, O. A., & Folagbade, S. O. (2026). Investigation of carbonation on the compressive strength development of Portland Limestone Cement concrete. Discover Civil Engineering, 3(1). https://doi.org/10.1007/s44290-026-00461-7

[19] Lemon, Md. M. R. (2026). Experimental Investigation on the Durability Properties of Concrete under Aggressive Environmental Conditions. Journal of Ceramics and Concrete Sciences, 11(1), 46-70. https://doi.org/10.46610/joccs.2026.v011i01.005

[20] Motlagh, S. A. T., & Naghizadehrokni, M. (2022). An extended multi-model regression approach for compressive strength prediction and optimization of a concrete mixture. Construction and Building Materials, 327, 126828. https://doi.org/10.1016/j.conbuildmat.2022.126828

[21] Loureiro, A. A. B., & Stefani, R. (2024). Comparing the performance of machine learning models for predicting the compressive strength of concrete. Discover Civil Engineering, 1(1). https://doi.org/10.1007/s44290-024-00022-w

[22] Sah, A. K., & Hong, Y.-M. (2024). Performance Comparison of Machine Learning Models for Concrete Compressive Strength Prediction. Materials, 17(9), 2075. https://doi.org/10.3390/ma17092075

[23] Bonagura, M. (2012). Nondestructive evaluation of concrete compression strength by means of Artificial Neural Network [University of Bologna]. In AMS Dottorato Institutional Doctoral Theses Repository. https://doi.org/10.6092/unibo/amsdottorato/4880

[24] Bonagura, M., & Nobile, L. (2021). Artificial Neural Network Approach for Predicting Concrete Compressive Strength by SonReb. Structural Durability & Health Monitoring, 15(2), 125-137. https://doi.org/10.32604/sdhm.2021.015644

[25] Trtnik, G., Kavčič, F., & Turk, G. (2008). Prediction of concrete strength using ultrasonic pulse velocity and artificial neural networks. Ultrasonics, 49(1), 53-60. https://doi.org/10.1016/j.ultras.2008.05.001

[26] Selçuk, S., & Tang, P. (2023). A metaheuristic-guided machine learning approach for concrete strength prediction with high mix design variability using ultrasonic pulse velocity data. Developments in the Built Environment, 15, 100220. https://doi.org/10.1016/j.dibe.2023.100220

[27] Shaaban, M. M., Amin, M. A., Selim, S. Z., & Riad, I. M. (2025). Machine learning approaches for forecasting compressive strength of high-strength concrete. Scientific Reports, 15(1), 25567. https://doi.org/10.1038/s41598-025-10342-1

[28] Elhishi, S., Elashry, A. M., & El-Metwally, S. (2023). Unboxing machine learning models for concrete strength prediction using XAI. Scientific Reports, 13(1), 19892. https://doi.org/10.1038/s41598-023-47169-7

[29] Akhtar, M. N., Husein Malkawi, D. A., & Albatayneh, O. (2026). Sustainable fine aggregate with SCMs-blends in structural concrete: A systematic research study. Results in Engineering, 32, 112265. https://doi.org/10.1016/j.rineng.2026.112265

[30] Waliitagi, A., Rathanasalam, V. S., Kishore, H. R. B., & Jeeva Chithambaram, S. (2023). The implications of sustainable fine aggregate on self-compacting concrete: A review. IOP Conference Series: Materials Science and Engineering, 1273(1), 012007. https://doi.org/10.1088/1757-899X/1273/1/012007

[31] Islam, Sk. R., Majumder, S. N., & Mutsuddy, R. (2024). Life cycle assessment and mechanical strength of cement composites with conventional, and recycled fine aggregate. Sustainable Structures, 4(2), 000052. https://doi.org/10.54113/j.sust.2024.000052

[32] Anupam, K., Akinmade, D., Kasbergen, C., Erkens, S., & Adebiyi, F. (2023). A state-of-the-art review of natural bitumen in pavement: Underlining challenges and the way forward. Journal of Cleaner Production, 382, 134957. https://doi.org/10.1016/j.jclepro.2022.134957

[33] Francis, D. O., Dayyabu, A., Aderinola, O. S., Kolo, M. U., Ijeoma, O. I., Akingbonmire, S. L., & Kolo, M. U. (2025). Potentials of bitumen tar sand for road work: A case study of Kajola, Lamudifa Irele LGA, Nigeria. Nile Journal of Engineering and Applied Science, 3(1). https://doi.org/10.5455/njeas.282386

[34] Akpan, U. G., David, Z., & Emena, A. (2024). Comparative study on the extraction strength of solvents on tar sand from Okitipupa, Ondo State. Nigerian Journal of Technology, 43(1), 51-55. https://doi.org/10.4314/njt.v43i1.7

[35] Olalekan, S. T., Arinkoola, A. O., Kolapo, S. K., Jimoh, M. O., Olufayo, A. O., Ayanshola, A. M., Ogunleye, O. O., & Abdulkareem, A. S. (2024). Durability of bitumen binder reinforced with polymer additives: Towards upgrading Nigerian local bitumen. Heliyon, 10(10), e30825. https://doi.org/10.1016/j.heliyon.2024.e30825

[36] Brand, A. S., & Roesler, J. R. (2016). Reclaimed asphalt pavement in concrete pavements: Properties, microstructure, and design. In Proceedings of the 11th International Conference on Concrete Pavements (pp. 946-963). https://doi.org/10.33593/iccp.v11i1.335

[37] Russo, N., Filippi, A., Carsana, M., Lollini, F., & Redaelli, E. (2025). Impact of RAP as recycled aggregate on durability-related parameters of structural concrete. Materials and Structures, 58, 53. https://doi.org/10.1617/s11527-025-02582-4

[38] Uygunoğlu, T., Topçu, İ. B., & Çınar, E. (2024). Durability effect of reclaimed asphalt aggregate on concrete road pavement. Materiales de Construcción, 74(353). https://doi.org/10.3989/mc.2024.356823

[39] Tiza, M. T., Agunwamba, J., & Okafor, F. (2024). Appraisal of reclaimed asphalt pavement as coarse aggregates in cement concrete. Environmental Research and Technology, 7(1), 27-40. https://doi.org/10.35208/ert.1320693

[40] Sanchaiwut, M., Thumrongvut, J., Pantawee, S., & Seangatith, S. (2022). Effects of substitution of fine aggregate with recycled asphalt pavement on compressive strength of normal concrete. Key Engineering Materials, 922, 163-168. https://doi.org/10.4028/www.scientific.net/KEM.922.163

[41] Chennuru, B., Deevi, V. B., Nallapati, J. N., Korampalli, R. H., Mallelli, P. V. B., Narendra Babu, P., & Kopuri, N. A. G. K. (2024). Experimental study on concrete by partial replacement of fine aggregate with bituminous road waste. International Journal of Engineering Research & Technology, 13(3). https://doi.org/10.17577/IJERTV13IS030020

[42] Anwar, A., Tariq, H., Adil, S., & Iftikhar, M. A. (2022). Effect of curing techniques on compressive strength of concrete. World Journal of Advanced Research and Reviews, 16(3), 694-710. https://doi.org/10.30574/wjarr.2022.16.3.1379

[43] Wang, Y., Xiao, R., Lu, H., Hu, W., Jiang, X., & Huang, B. (2023). Effect of curing conditions on the strength and durability of air-entrained concrete with and without fly ash. Cleaner Materials, 7, 100170. https://doi.org/10.1016/j.clema.2023.100170

[44] Ram, S., Dengri, A., & Kumar, R. (2024). Assessment of compressive strength in ordinary Portland cement concrete: A study of curing methods and duration. Evergreen, 11(2), 640-651. https://doi.org/10.5109/7183321

[45] Ferreira, R. L. S., Medeiros, M., Pereira, J. E. S., Henriques, G. F., Tavares, J. C., Marvila, M. T., & de Azevedo, A. R. G. (2023). Effects of particle size distribution of standard sands on the physical-mechanical properties of mortars. Materials, 16(2), 844. https://doi.org/10.3390/ma16020844

[46] Paudel, S., Pudasaini, A., Shrestha, R. K., & Kharel, E. (2023). Compressive strength of concrete material using machine learning techniques. Cleaner Engineering and Technology, 15, 100661. https://doi.org/10.1016/j.clet.2023.100661

[47] Sivakarthi, G., Viknesh, S. R., & Ram, S. Y. (2025). AI-driven multi-model prediction of concrete compressive strength using ANN, XGBoost, and random forest.

[48] Almutairi, A. (2025). Explainable machine learning-based prediction of compressive strength in sustainable recycled aggregate self-compacting concrete using SHAP analysis. Sustainability, 17(24), 11334. https://doi.org/10.3390/su172411334

[49] Ahmed, A. H. A., Jin, W., & Ali, M. A. H. (2024). Prediction of compressive strength of recycled concrete using gradient boosting models. Ain Shams Engineering Journal, 15(9), 102975. https://doi.org/10.1016/j.asej.2024.102975

[50] Al Adnan, M., Babur, M., Farooq, F., Shahid, M., Ahmed, Z., & Das, P. (2025). Prediction of splitting tensile strength of fiber-reinforced recycled aggregate concrete utilizing machine learning models with SHAP analysis. Hybrid Advances, 11, 100507. https://doi.org/10.1016/j.hybadv.2025.100507

[51] Zhang, Z., Luo, B., & Su, Y. (2026). Machine learning-based prediction of compressive strength in recycled aggregate self-compacting concrete: An ensemble modeling approach with SHAP interpretability analysis. Applied Sciences, 16(5), 2432. https://doi.org/10.3390/app16052432

[52] Kim, J. (2025). Challenges with hard-to-learn data in developing machine learning models for predicting the strength of multi-recycled aggregate concrete. Applied Soft Computing, 113110. https://doi.org/10.1016/j.asoc.2025.113110

[53] Padavala, S. S. A. B., Kothuri, D., & Gashe, A. M. (2026). Explainable machine learning-based optimization of strength, durability, and carbon efficiency of fly ash-GGBS geopolymer concrete. Scientific Reports, 16. https://doi.org/10.1038/s41598-026-48502-6

[54] Pap, M., Mahler, A., Illés, Z., Nehme, S. G., & Biró, A. (2025). Comparative assessment of pore structure and water retention in concrete using MIP, CT, SEM, and dewpoint techniques. Periodica Polytechnica Civil Engineering, 69(4), 1203-1215. https://doi.org/10.3311/ppci.41892

[55] Arora, S., Jangra, P., Lim, Y. Y., & Pham, T. M. (2023). Strength, durability, and microstructure of self-compacting geopolymer concrete produced with copper slag aggregates. Environmental Science and Pollution Research, 30, 666-684. https://doi.org/10.1007/s11356-022-22170-1

[56] Bilgehan, M., & Turğut, P. (2010). Artificial neural network approach to predict compressive strength of concrete through ultrasonic pulse velocity. Research in Nondestructive Evaluation, 21(1), 1-17. https://doi.org/10.1080/09349840903122042

[57] Collivignarelli, M. C., Cillari, G., Ricciardi, P., Miino, M. C., Torretta, V., Rada, E. C., & Abbà, A. (2020). The production of sustainable concrete with the use of alternative aggregates: A review. Sustainability, 12(19), 7903. https://doi.org/10.3390/su12197903

[58] Berriache, A., Bensoula, M., Zaoui, M., & Kadri, T. (2023). Study and valorization of a new bituminous concrete based on natural dune sand for hot and arid environments. The Journal of Engineering and Exact Sciences, 9(12), 17791. https://doi.org/10.18540/jcecvl9iss12pp17791

[59] Chou, J.-S., Chiu, C.-K., Farfoura, M., & Al-Taharwa, I. (2011). Optimizing the prediction accuracy of concrete compressive strength based on a comparison of data-mining techniques. Journal of Computing in Civil Engineering, 25(3), 242-253. https://doi.org/10.1061/(ASCE)CP.1943-5487.0000088